High-pressure synthesis of the double perovskite Sr_2FeMoO_6: increment of the cationic ordering and enhanced magnetic properties

2009 J. Phys.: Condens. Matter 21 186003

(http://iopscience.iop.org/0953-8984/21/18/186003)

J. Phys.: Condens. Matter **21** (2009) 186003 (6pp) doi:10.1088/0953-8984/21/18/186003

High-pressure synthesis of the double perovskite Sr_2FeMoO_6: increment of the cationic ordering and enhanced magnetic properties

M Retuerto, M J Martínez-Lope, M García-Hernández and J A Alonso

Instituto de Ciencia de Materiales de Madrid, CSIC, Cantoblanco, E-28049 Madrid, Spain

Received 17 February 2009, in final form 10 March 2009
Published 6 April 2009
Online at stacks.iop.org/JPhysCM/21/186003

Abstract

The double perovskite Sr_2FeMoO_6 has been prepared in polycrystalline form by high-pressure methods, starting from a precursor developed via a citrate technique, containing an elevated degree of anti-site disordering. The application of high external pressure (2 GPa) to Sr_2FeMoO_6 promotes the long distance Fe/Mo cationic order, due to the smaller lattice volume of the ordered sample. Both the disordered perovskite obtained at ambient pressure and the sample synthesized under high-pressure methods have been characterized by means of x-ray diffraction, neutron powder diffraction and magnetic measurements. The magnetic properties of the two oxides have been compared; the specimen prepared under high pressure not only presents an improved cationic ordering, but also displays a superior saturation magnetization and a sharpener ferromagnetic transition at a significantly high temperature of 430 K.

(Some figures in this article are in colour only in the electronic version)

1. Introduction

A decade ago, Kobayashi *et al* [1] reported the half-metallicity and ferromagnetism ($T_C \sim 400$ K) of Sr_2FeMoO_6 double perovskite, which also presents substantial low-field magnetoresistance (LFMR) at room temperature. The rising interest in the half-metallic systems is mainly due to their potential applications in spintronics, since junctions made of half-metals should ideally present infinite magnetoresistance ratios or 100% spin polarized currents, and they could be used in a panoply of magnetic devices including non-volatile MRAM, hybrid spintronic devices, and in hard drive read head sensor elements. While the well-known doped manganites exhibit low Curie temperatures and one requires high magnetic fields to obtain an appreciable negative magnetoresistance response from these systems, the double perovskites of the family $A_2BB'O_6$ (A = alkaline earth; B, B′ = transition metals) are appealing since they have highly spin polarized conduction bands and Curie temperatures above RT. Moreover, the double perovskites are also of fundamental interest since neither their basic physics nor their material aspects are very well understood.

The ideal structure of Sr_2FeMoO_6 can be viewed as a regular arrangement of corner-sharing FeO_6 and MoO_6 octahedra, alternating along the three directions of the crystal, with the voluminous Sr cations occupying the voids in between the octahedra. In a simple picture, the ferrimagnetic structure can be described as an ordered array of parallel Fe^{3+} ($S = 5/2$) magnetic moments, antiferromagnetically coupled with Mo^{5+} ($S = 1/2$) spins. In this ideal model, the saturation magnetization, at low temperature, would be 4 μ_B per formula unit (fu).

In the real world, such a large magnetization value has not been obtained for bulk Sr_2FeMoO_6. Ogale *et al* [2], using Monte Carlo simulation, examined the influence in the magnetization of the so-called anti-site B cation disorder, implying that some Mo^{5+} cations occupy the positions of Fe^{3+} cations ('anti-site disorder') and vice versa. During the last few years many efforts have been addressed to understanding the effects of the 'anti-site disorder' in the

magnetic and transport properties. It is well known that the intensity of the ferromagnetic interactions decreases when the disorder increases, disturbing the magnetic order temperature and the saturation magnetization [3–5]. In addition, predictions based upon band structure calculations suggest that the disorder modifies the band structure of the material by partially suppressing the spin polarization and reducing the half-metallic and ferromagnetic characteristics of the compound [6, 7].

Sr_2FeMoO_6 has been extensively studied. In 1999 Kim *et al* [8] reported intergranular magnetoresistance at room temperature, and García-Landa *et al* [9] synthesized the material using solid state methods. Many other papers have been focused on the increase of the anti-site disorder. Niebieskikwiat *et al* [10], using solid state methods, obtained a material with $M_S = 2.7\ \mu_B$ and $T_C \sim 405$ K. Chmaissem *et al* [11] also prepared this material by solid state synthesis and subsequently reduction in a 1%/99% H_2/Ar flow at high temperatures, describing a compound with 4% of the Fe cations over the Mo positions and $M_S = 3.6\ \mu_B$. Martínez *et al* [12] and Navarro *et al* [13] were able to develop Sr_2FeMoO_6 with only 2% cationic disorder, $M_S = 3.75\ \mu_B$ and $T_C \sim 420$ K. In a previous work, using wet chemistry methods, we prepared Sr_2FeMoO_6 in almost completely ordered form with $M_S = 3.98\ \mu_B$ and record magnetoresistance at room temperature [14].

It is well known that in the double perovskites $A_2BB'O_6$ the long range ordering between B and B′ cations is primarily determined by the differences between the charges and ionic radii of B and B′ ions. For a given set of cations, the degree of ordering between Fe and Mo depends mainly on the synthesis conditions; as a rule of thumb, increased order may be obtained with higher synthesis temperatures [5] or longer treatment times [15]. In this work we try to increase the degree of cationic order using high-pressure methods. The high-pressure conditions favor the formation of phases with smaller lattice volume which implies compression of the chemical bonds. Considering a structural transformation induced by a pressure from F_1 to F_2 (F being a structural form), due to the compressibility, the value of the difference in volume, ΔV, between the two forms must be negative:

$$\left[\Delta V = \sum (V/Z)_{F_2} - (V/Z)_{F_1}\right]$$

(where V is the unit-cell volume and Z is the number of formula units per unit cell). Under high-pressure conditions only structural transformation characterized by a negative ΔV value can take place.

Perfectly ordered double perovskites present smaller unit-cell volumes than anti-site disordered structures, since the cationic disorder at the B positions generates regions where sets of adjacent highly charged cations give rise to an additional repulsion that increases the average volume of the compound. In the case of Sr_2FeMoO_6, a neutron powder diffraction (NPD) study of samples with different degrees of ordering demonstrated that the disordered material exhibits a considerable volume over a wide temperature interval [4]. Therefore, we thought that the application of external pressure to a partially disordered sample, at sufficiently high temperatures to allow the cationic motion, would help to modify the Fe and Mo cation arrangement, promoting the long range cationic ordering, thus involving a reduction of the cationic repulsion, shorter chemical bonds, and consequently smaller unit-cell volumes.

2. Experimental details

We synthesized a partially disordered sample of Sr_2FeMoO_6 by a soft chemistry procedure, designed to obtain very reactive precursors, by dissolving stoichiometric amounts of $Sr(NO_3)_2$, $FeC_2O_4{\cdot}2H_2O$ and $(NH_4)_6Mo_7O_{24}{\cdot}4H_2O$ in citric acid. The citrate and nitrate solutions were slowly evaporated, leading to organic resins that contain a homogeneous distribution of the cations involved. The resins were dried at 120 °C and then decomposed at 600 °C for 12 h. The organic materials and nitrates were eliminated in a subsequent treatment at 800 °C in air, for 2 h. This treatment gave rise to finely divided and homogeneous precursor materials. Then, the precursors were ramped at 5 °C min $^{-1}$ up to 850 °C and annealed at this temperature for 2 h in H_2/N_2 (5%/99%) reducing flow. In this way we obtained the disordered sample, called hereafter the 'ambient-pressure' sample.

The 'ambient-pressure' sample was introduced into a gold capsule and placed in a cylindrical graphite heater to synthesize another sample under high-pressure conditions (called hereafter the 'high-pressure' sample). The reaction was carried out in a piston–cylinder press (Rockland Research Co.), at a pressure of 2 GPa and at 800 °C for 60 min. The raw product, obtained as a dense homogeneous pellet, was ground to perform x-ray and neutron diffraction and magnetic characterization.

Both samples were characterized by means of x-ray diffraction (XRD) (Cu Kα_1, $\lambda = 1.54056(1)$ Å). Anti-site disorder at the B positions was determined by Rietveld refinement from XRD data. Neutron powder diffraction (NPD) experiments were carried out using the high-resolution powder diffractometer D2B ($\lambda = 1.594(2)$ Å) at the ILL, Grenoble, for the 'high-pressure' sample. The patterns were collected at 2 K, room temperature (295 K) and 450 K, in the paramagnetic regime. The crystal structures were refined with the FULLPROF Rietveld refinement program [16], keeping the degree of B-site ordering fixed at the value obtained from the XRD. The dc magnetic susceptibility measurements were carried out using a commercial (Quantum Design) SQUID magnetometer in the temperature range from 2 to 700 K.

3. Results and discussion

Sr_2FeMoO_6 samples were obtained as black, well-crystallized powders. A single-phase tetragonal perovskite was identified for both materials: the 'ambient-pressure' sample and the 'high-pressure' sample. Figure 1 shows the laboratory XRD diagrams at RT. Both patterns show superstructure peaks arising from the Fe/Mo ordering (e.g., (011) and (013)). The degree of Fe/Mo ordering is defined as d.o. $= (1 - as)100$, where the parameter *as* (anti-site disorder) is the fraction of Mo

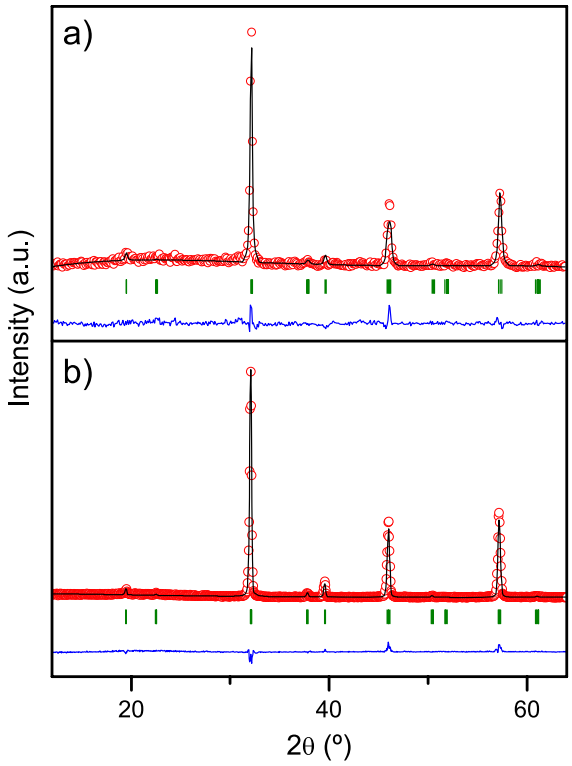

Figure 1. Observed (circles), calculated (full line) and difference (bottom) XRD Rietveld profiles of Sr_2FeMoO_6; (a) 'ambient-pressure' sample and (b) 'high-pressure' sample.

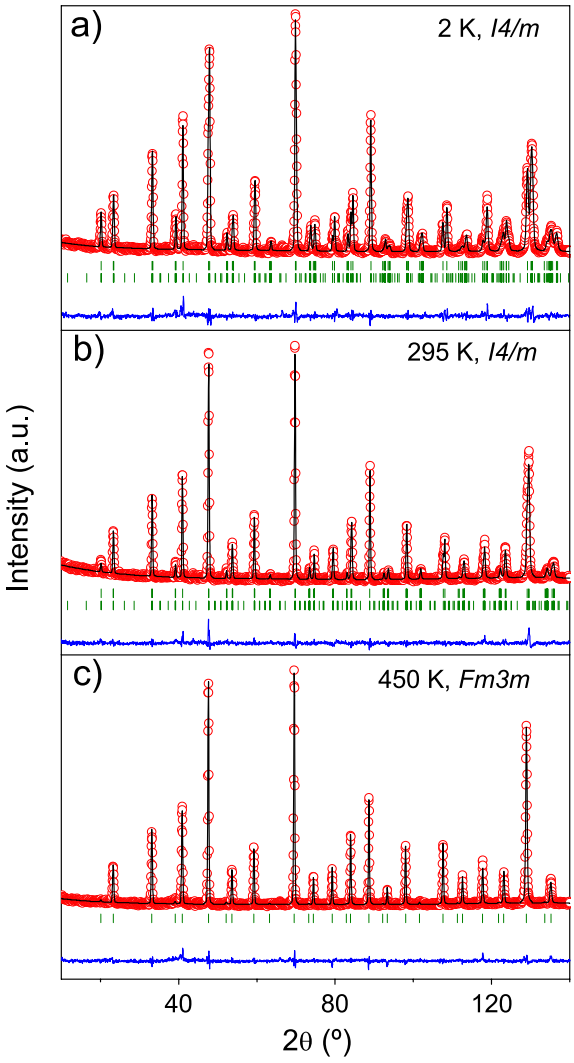

Figure 2. Observed (circles), calculated (full line) and difference (bottom) NPD Rietveld profiles at (a) 2 K, (b) 295 K and (c) 450 K for the 'high-pressure' sample. The two sets of reflection markers (vertical bars) in (a) and (b) correspond to the crystallographic and magnetic structures, respectively.

atoms at Fe positions; notice that *as* would take a value of 0.5 for a completely disordered sample. From the analysis of the intensities of these reflections, via Rietveld refinements of the XRD data, the degree of ordering was estimated to be 65% for the 'ambient-pressure' sample and 89% for the 'high-pressure' Sr_2FeMoO_6 specimen.

A NPD study was useful for investigating the structural details of Sr_2FeMoO_6 for the 'high-pressure' sample, from the 2, 295 and 450 K NPD patterns collected at the D2B diffractometer. The refinement of the crystal structure was performed by the Rietveld method. At RT the crystal structure was defined in the $I4/m$ space group (No. 87), $Z = 2$, with unit-cell parameters related to a_0 (ideal cubic perovskite, $a_0 \approx 3.9$ Å) as $a = b \approx \sqrt{2}a_0$, $c \approx 2a_0$; in the present case $a = 5.570\,43(7)$ Å, $c = 7.8978(1)$ Å. Sr atoms were located at 4d (0, 1/2, 1/4) positions, Fe at 2a (0, 0, 0), Mo at 2b (0, 0, 1/2) sites, and oxygen atoms O1 at 4e (0, 0, z) and O2 at 8h (x, y, 0) positions. The degree of anti-site disorder was fixed at the value obtained by the Rietveld analysis of the XRD pattern. At 2 K the structure was also refined in the $I4/m$ space group. Both 2 K and RT refinements were completed after the introduction of the magnetic contribution arising for Fe and Mo moments, which are magnetically ordered even above RT. The 2 K and RT NPD data reveal a strong magnetic contribution to the low-angle reflections, especially visible at the [011] Bragg position, at ≈20.5°. A ferrimagnetic structure was modeled with magnetic moments at the Fe and Mo positions coupled antiferromagnetically. The magnetic structure can be described as a ferrimagnetic arrangement of Fe and Mo moments lying along the [001] direction. The refined magnetic moments for Fe and Mo are 2.3(7) μ_B and −0.4(7) μ_B at RT and 3.8(1) μ_B and −0.44(9) μ_B at 2 K, respectively. Figures 2(a) and (b) illustrate the quality of the fit between observed and calculated NPD profiles for the 'high-pressure' sample at 2 K and 295 K, respectively.

At 450 K the structure was refined in the cubic $Fm\bar{3}m$ space group (No. 225), with a doubled unit-cell parameter $c \approx 2a_0$, $Z = 4$. Figure 2(c) shows the goodness of the fit for the 450 K NPD pattern. Table 1 summarizes the structural parameters at 2, 295 and 450 K: atomic coordinates, lattice parameters, volume and isotropic temperature factors, as well as the reliability factors after the Rietveld refinements. Table 2 includes the interatomic distances and some selected bond angles. The structural results completely agree with those published by Chmaissem *et al* [11] reporting a tetragonal to cubic structure transition concomitant with the ferromagnetic transition (T_C). The high-temperature structure (above T_C)

Table 1. Atomic parameters and agreement factors after the Rietveld refinement of the crystal structure of the 'high-pressure' Sr_2FeMoO_6 sample from NPD data collected at 2, 295 and 450 K; space groups $I4/m$, $I4/m$ and $Fm3m$, respectively.

T (K)	2	295		450
$I4/m$			$Fm3m$	
a (Å)	5.5520(1)	5.570 43(7)	a (Å)	7.9012(1)
c (Å)	7.9029(2)	7.8978(1)	V (Å^3)	493.27(1)
V (Å^3)	243.609(8)	245.068(7)		
Sr 4d(0 1/2 1/4)			Sr 8c(1/4 1/4 1/4)	
B (Å^2)	0.17 (3)	0.62(3)	B (Å^2)	0.97(2)
Fe 2a(0 0 0)			Fe 4a(0 0 0)	
B (Å^2)	−0.11(1)	1.28(1)	B (Å^2)	0.39(6)
Magnetic moment (μ_B)	3.8(1)	2.3(7)		
Mo 2b(0 0 1/2)			Mo 4b(1/2 1/2 1/2)	
B (Å^2)	0.24(2)	−1.26(2)	B (Å^2)	0.14(8)
Magnetic moment (μ_B)	−0.44(9)	−0.4(7)		
Occupancy[a]				
Fe (2a)	0.89(1)	0.89(1)		0.89(1)
Mo (2a)	0.11(1)	0.11(1)		0.11(1)
O1 4e(0 0 z)			O 24e(x 0 0)	
z	0.2550(4)	0.2521(6)	x	0.2521(2)
B (Å^2)	0.21(6)	0.65(8)	B (Å^2)	1.12(1)
O2 8h(x y 0)				
x	0.2769(3)	0.2703(4)		
y	0.2254(3)	0.2338(4)		
B (Å^2)	0.23(4)	0.82(4)		
Reliability factors			Reliability factors	
χ^2	1.96	1.24	χ^2	1.70
R_p (%)	5.86	4.40	R $_p$ (%)	5.85
R_{wp} (%)	7.75	5.58	R_{wp} (%)	7.73
R_I (%)	5.54	5.02	R_I (%)	5.92
R_{mag} (%)	7.01	3.17		

[a] The Fe/Mo occupancy factors were determined from XRD data and fixed in the refinement of the NPD data.

Table 2. Some selected bond lengths (Å) and angles (deg) for Sr_2FeMoO_6 at 2, 295 and 450 K.

Temperature	2 K	295 K	Temperature	450 K
FeO_6 octahedra			FeO_6 octahedra	
Fe–O_1 ($x2$)	2.015(5)	1.999(6)	Fe–O	1.992(3)
Fe–O_2 ($x4$)	1.982(3)	1.995(3)		
⟨Fe–O⟩	1.998(4)	1.997(5)		
MoO_6 octahedra			MoO_6 octahedra	
Mo–O_1 (x 2)	1.936(5)	1.950(6)	Mo–O	1.959(3)
Mo–O_2 (x 4)	1.964(3)	1.955(3)		
⟨Mo–O⟩	1.950(4)	1.953(5)		
Fe–O1–Mo	180.0	180.0	Fe–O–Mo	180.0
Fe–O2–Mo	168.2(1)	171.5(1)		
Bond valences			Bond valences	
Fe	2.98(1)	2.97(1)	Fe	2.99(1)
Mo	5.27(2)	5.29(2)	Mo	5.22(1)

crystallizes in the $Fm\bar{3}m$ space group, which contains a rock-salt like distribution of Fe and Mo cations over the B sublattice positions, in perfectly ordered samples, and implies an Fe–O–Mo angle of 180°. In the ferromagnetic region, the tetragonal structure can be described as a result of a single anti-phase octahedral tilting along the c axis. The magnitude of this tilting can be simply derived from the Fe–O2–Mo angle as

$$\Phi = \frac{180 - \langle \text{Fe–O2–Mo} \rangle}{2}.$$

This angle evolves from a maximum value of $\Phi = 5.9(2)°$ at 2 K, to $\Phi = 4.2(4)°$ at 295 K and finally to $\Phi = 0$ at 450 K, at the onset of the structural phase transition from tetragonal (low temperature) to cubic (high temperature). Figure 3 shows the thermal variation of Φ mapping out a phase diagram of this system; a schematic view of the tetragonal and cubic structures is also displayed.

At 2 K, the FeO_6 and MoO_6 octahedra present a slight axial distortion (elongated and compressed along the c axis, respectively), which is virtually negligible at 295 K, within the standard deviations. At 450 K, in the cubic phase, both Fe and Mo octahedra are perfectly regular. The average ⟨Fe–O⟩ and ⟨Mo–O⟩ bond lengths, of 1.998(4) and 1.950(4) Å at 2 K, are considerably different from those given by Sánchez *et al* [4] for a disordered sample, of 1.97(5) and 1.98(5) Å, at 15 K, where both types of octahedra are virtually equal; this difference is a consequence of the more complete Fe/Mo ordering in the 'high-pressure' sample, since a complete disordering tends to homogenize B–O and B′–O distances.

Brown's phenomenological bond-valence model (BVS) [17] can also help to give an estimation of the actual valences

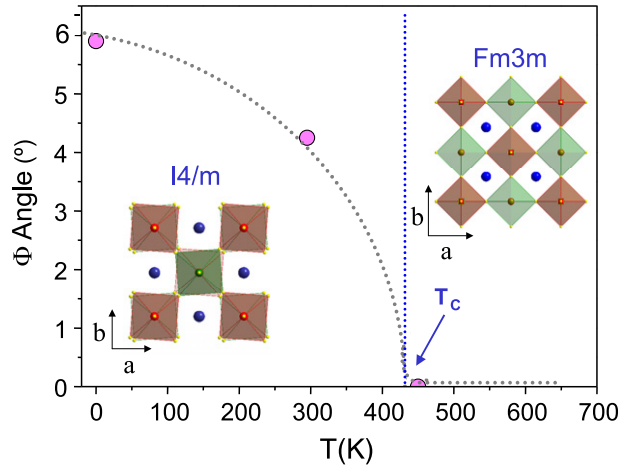

Figure 3. Thermal evolution of the Φ angle characterizing the anti-phase rotation of the FeO_6 and MoO_6 octahedra along the *c* axis. In this phase diagram the T_C temperature defines the limits between the low-temperature tetragonal phase and high-temperature cubic structure.

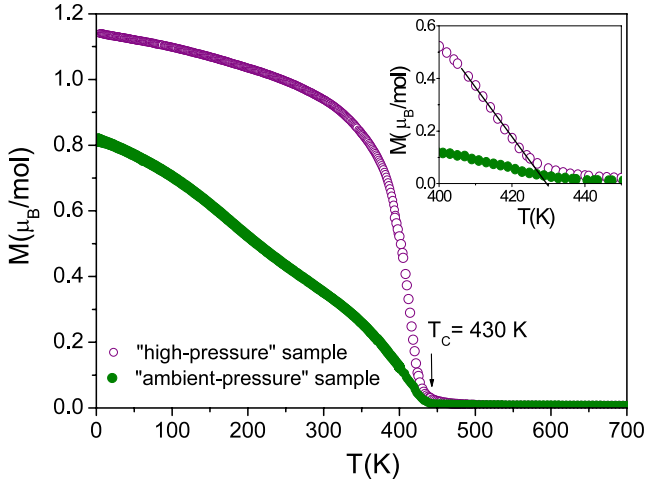

Figure 4. dc-magnetic susceptibility as a function of temperature of 'ambient-pressure' and 'high-pressure' Sr_2FeMoO_6 samples. Inset: close-up in the 400–450 K region.

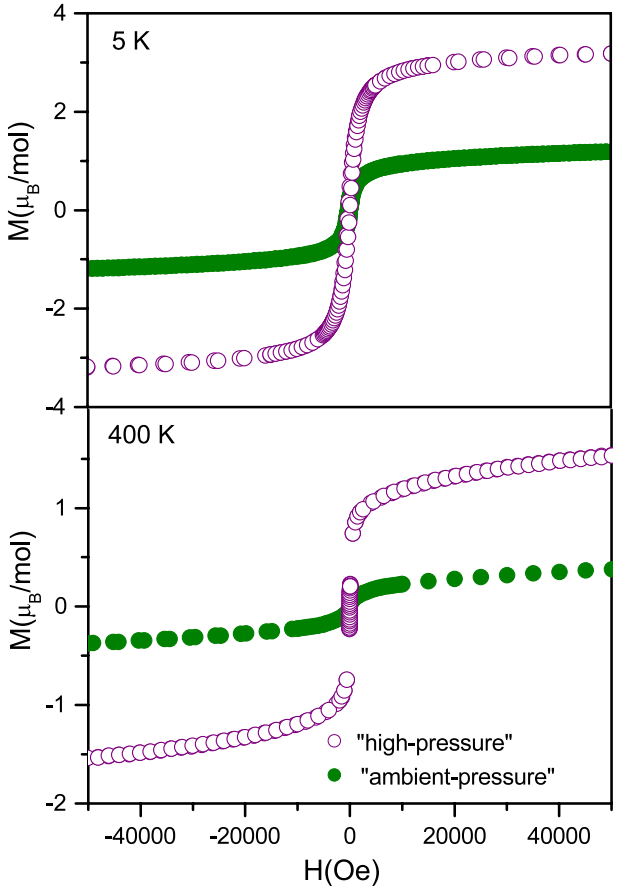

Figure 5. Magnetization versus magnetic field at 5 and 400 K for 'ambient-pressure' and 'high-pressure' Sr_2FeMoO_6 samples with 65% and with 89% cationic ordering, respectively.

on the cations and anions of a given structure, by means of an empirical relationship between the observed bond lengths and the valence of a bond. Table 2 includes the values of the bond valences of Fe and Mo that exhibit intermediate oxidation states, as expected, although the present results suggests an electronic configuration close to $Fe^{3+}(3d^5)$–$Mo^{5+}(4d^1)$, showing a negligible temperature evolution.

The dc magnetic susceptibility curves (figure 4) for the 'ambient-pressure' sample with 65% cationic ordering and the 'high-pressure' sample with 89% cationic ordering exhibit a spontaneous increase of the magnetization upon cooling, characteristic of a ferromagnet. The ferromagnetic transition is considerably sharper for the 'high-pressure' sample; by contrast the 'ambient-pressure' sample presents a broad transition that does not reach saturation even at very low temperatures. The Curie temperature for the 'high-pressure' sample is 430 K, as shown in the inset of figure 4; it is among the highest T_C temperatures ever reported for Sr_2FeMoO_6 double perovskite [13, 18], although below the record value of 440 K [19]. However, for the 'ambient-pressure' sample, with 65% Fe/Mo ordering, T_C is difficult to estimate due to the broadness of the magnetic transition from paramagnetic to ferromagnetic.

From the magnetization versus magnetic field data at 5 and 400 K represented in figure 5 we obtained a saturation magnetization at 5 K of $M_S = 1.18\ \mu_B$/fu for the 'ambient-pressure' sample and $M_S = 3.2\ \mu_B$/fu for the 'high-pressure' sample. Even at 400 K we observe saturation magnetizations of 0.38 μ_B/fu and 1.54 μ_B/fu for the 'ambient-pressure' and 'high-pressure' samples, respectively. The disordered 'ambient-pressure' sample presents smaller saturation magnetization due to the larger number of Fe-rich patches, with antiferromagnetic arrangement of the Fe magnetic moments, which decrease the saturation magnetization. For the 'high-pressure' sample the saturation magnetization is significant at 400 K, since the compound is still ferromagnetic at this temperature. At higher temperatures both samples become paramagnetic.

The enhancement of the T_C temperature in a Sr_2FeMoO_6 sample obtained under high-pressure conditions deserves some discussion. In this sample, the saturation magnetization takes moderate values of $M_S = 3.2\ \mu_B$/fu, since there is a non-negligible amount of anti-site disordering. The mechanism that

accounts for the high T_C is certainly related to an improvement of the magnetic interactions between Fe and Mo atoms. In this sense, it has been proposed [20] that the magnetic interactions in Sr_2FeMoO_6 are mediated by itinerant electrons in π^* bands coming from t_{2g} orbitals of Mo origin. In this way, it is thought that an increment in the number of carriers in the spin polarized conduction band would induce an enhancement of T_C. This increase has been effectively achieved by trivalent cation substitutions at Sr^{2+} sites (electron doping), as reported for the series $Sr_{2-x}La_xFeMoO_6$ [21, 22] and $Sr_{2-x}Ce_xFeMoO_6$ [23]. Experimentally, it is found that in electron-doped samples there is a net decrease of the Mo valence upon electron doping, concomitant with a reinforcement of the magnetic interactions. In the present case, it is interesting to compare the Fe and Mo valences determined from the NPD study for the high-pressure sample with those obtained for Sr_2FeMoO_6 samples prepared by the standard procedure involving treatments at high temperatures under reducing conditions (H_2 flow). The bond-valence values for Fe and Mo in a sample with a notably high T_C value of 416 K [14] are 2.91(2)+ and 5.38(3)+, respectively, at RT. In the present case, the high-pressure sample exhibits bond-valence values for Fe and Mo of 2.97(1)+ and 5.29(2)+, respectively, at RT (table 2). In this latter sample there seems to be a redistribution of the electronic cloud, perceptibly incrementing the electronic density on the Mo site, in the same manner as was observed for the aforementioned series of electron-doped materials with enhanced T_Cs. It is evident that the equilibrium mixed valence displayed by Sr_2FeMoO_6, intermediate between the extreme configurations $Fe^{3+}(3d^5)$–$Mo^{6+}(4d^0)$ and $Fe^{2+}(3d^6)$–$Mo^{5+}(4d^1)$ [24], subtly depends on the external conditions such as temperature, pressure, atmosphere, etc. Given the different compressibilities of the Mo–O and Fe–O bonds, we suggest that the external pressure applied during the synthesis process shifts the oxygen positions and thus the electronic cloud across Fe–O–Mo paths, incrementing the oxidation state of Fe cations at the expense of reducing the valence of Mo atoms. The quenching of the high-pressure phase allows stabilizing at ambient conditions the equilibrium atomic positions existing under high pressure. As a collateral effect, the electronic shift towards the Mo sites enhances the magnetic interactions and it realizes an effective increment of the Curie temperature.

4. Conclusion

We have demonstrated that the application of an external pressure in the 2 GPa range, at sufficiently high temperatures (800 °C in this case), is an effective way to increase the long distance cationic ordering in double perovskites, due to the smaller unit-cell volume presented by the ordered samples. As a consequence of the reduction of the unwanted anti-site Fe/Mo disordering, the 'high-pressure' sample displays optimized magnetic properties, as far as T_C and the saturation magnetization are concerned, with respect to the precursor perovskite with lower degree of ordering. The observed increment of T_C is correlated with the bond valences determined for Fe and Mo from the structural data; the shift of the electronic cloud towards Mo, observed also in electron-doped samples, seems to account for the enhancement of the magnetic interactions of the high-pressure material.

Acknowledgments

We thank the Spanish Ministry of Education for the financial support of the project MAT2007-60536 and we are grateful to ILL for making all facilities available.

References

[1] Kobayashi K-I, Kimura T, Sawada H, Terakura K and Tokura Y 1998 *Nature* **395** 677
[2] Ogale A S, Ogale S B, Armes R and Venkatesan T 1999 *Appl. Phys. Lett.* **75** 0537
[3] Navarro J, Nogues J, Muñoz J S and Fontcuberta J 2003 *Phys. Rev.* B **67** 174416
[4] Sanchez D, Alonso J A, García-Hernández M, Martinez-Lope M J and Martínez J L 2002 *Phys. Rev.* B **65** 104426
[5] Balcells L, Navarro J, Bibes M, Roig A, Martínez B and Fontcuberta J 2001 *Appl. Phys. Lett.* **78** 781
[6] Saha-Dasgupta T and Sarma D D 2001 *Phys. Rev.* B **64** 064408
[7] Stoeffler D and Colis S 2005 *J. Magn. Magn. Mater.* **290** 400
[8] Kim T H, Uehara M, Cheong S-W and Lee S 1999 *Appl. Phys. Lett.* **74** 1737
[9] García-Landa B, Ritter C, Ibarra M R, Blasco J, Algarabel P A, Mahendiran R and García J 1999 *Solid State Commun.* **110** 435
[10] Niebieskikwiat D, Sánchez R D, Caneiro A, Morales L, Vásquez-Mansilla M, Rivadulla F and Hueso L E 2000 *Phys. Rev.* B **62** 3340
[11] Chmaissem O, Kruk R, Dabrowski B, Brown D E, Xiong X, Kolesnik S, Jorgensen J D and Kimball C W 2000 *Phys. Rev.* B **62** 14197
[12] Martínez B, Navarro J, Balcells L and Fontcuberta J 2000 *J. Phys.: Condens. Matter* **12** 10515
[13] Navarro J, Frontera C, Balcells Ll, Martínez B and Fontcuberta J 2001 *Phys. Rev.* B **64** 092411
[14] Retuerto M, Alonso J A, Martínez-Lope M J, Martínez J L and García-Hernández M 2004 *Appl. Phys. Lett.* **85** 266
[15] Woodward P, Hoffmann R D and Sleight A W 1994 *J. Mater. Res.* **9** 2118
[16] Rodriguez-Carvajal J 1993 *Physica* B **192** 55
[17] Brese N E and O'Keefe M 1991 *Acta Crystallogr.* B **47** 192
[18] Borges R P, Thomas R M, Cullinan C, Coey J M D, Surynarayanan R, Ben-Dor L, Gaudart L P and Revcolevski A 1999 *J. Phys.: Condens. Matter* **11** L445
[19] Ritter C, Blasco J, De Teresa J M, Serrate D, Morellon L, Garcia J and Ibarra M R 2004 *Solid State Sci.* **6** 419
[20] Sarma D D, Mahadevan P, Saha-Dasgupta T, Sugata R and Ashwani K 2000 *Phys. Rev. Lett.* **85** 2549
[21] Serrate D, De Teresa J M, Blasco J, Ibarra M R, Morellón L and Ritter C 2002 *Appl. Phys. Lett.* **80** 4573
[22] Sánchez D, Alonso J A, García-Hernández M, Martínez-Lope M J, Casais M T and Martínez J L 2003 *J. Mater. Chem.* **13** 1771
[23] Retuerto M, Alonso J A, Martínez-Lope M J, Menéndez N, Tornero J and García-Hernández M 2006 *J. Mater. Chem.* **16** 865
[24] Linden J, Yamamoto T, Karppinen M, Yamauchi H and Pietari T 2000 *Appl. Phys. Lett.* **76** 2925